Application of HOSVD to Aerodynamics. The Problem of Shock Waves.

L. S. Lorente , D. Alonso , J. M. Vega and A. Velazquez

Aerospace Propulsion and Fluid Mechanics Department, School of Aeronautics, Universidad Politécnica de Madrid

Applied Mathematics Department, School of Aeronautics, Universidad Politécnica de Madrid

emails: luissantiago.lorente@upm.es, diego.alonso.fernandez@upm.es, josemanuel.vega@upm.es, angel.velazquez@upm.es

Abstract

Efficient interpolation in aerodynamic databases is important for the aeronautic industry because of its implication on both the cost and time needed to complete design cycles. In this study a method based on high-order singular value decomposition is presented focusing on the problems associated with the shock wave like structures that do not suit well with this kind of methods. To illustrate the methodology, the flow around a two-dimensional airfoil is considered at a Reynolds number of 20×10^6 with three free parameters, namely, the Mach number, the angle of attack, and the flap deflection angle in the ranges of $[0.4, 0.8]$, $[-3°, 3°]$, and $[-5°, 5°]$, respectively. The method is robust in the sense of being able to deal with very different flow topologies.

Key words: SVD, HOSVD, shock waves, aerodynamic coefficients

1 Introduction

Nowadays, the use of Computational Fluid Dynamics (CFD) is widespread in the aeronautic industry. One of the many aspects to be dealt with in the context of aerodynamics design is database generation. Usually, these databases are multiparametric, and thousands of computer runs are needed to fill them up. But accuracy degrades when either more than a few parameters are involved or the distance between the available points in the parametric space is not small enough. An alternative method to plain interpolation, proposed by Bui-Thanh [1], consists of the combined use of interpolation and techniques based on either singular value decomposition (SVD) or proper orthogonal decomposition (POD): interpolation is carried out using SVD or POD modes that

already contain global information of the whole parametric space instead of doing it locally. However, one of the difficulties associated with the use of the SVD/POD formulations in their original form is that they are not well suited to deal with flow topologies that present shock wavelike structures. In this context, the main objective of this study is to present a method focused on the generation of aerodynamic databases containing airfoil flowfields that exhibit pressure and/or a suction side shock wave and large separated flow regions. The method is based on high-order singular value decomposition (HOSVD), which is a recent generalization of SVD to the case of parametric spaces having more than two dimensions. Further information on the results below can be found in [2].

2 High-Order Singular Value Decomposition

HOSVD is an extension of SVD [3] (which only applies to matrices) to third or larger order tensors. The SVD of a matrix A provides a decomposition of the elements of A in the form

$$A_{ij} = \sum_{l=1}^{r} \delta_l u_{il} v_{jl}, \tag{1}$$

where δ_l are the singular values and, for each value of subscript l, u_{il} and v_{il} are the SVD modes of matrix A. The latter are the eigenvectors associated with the nonzero eigenvalues of the symmetric matrices $A \cdot A^T$ and $A^T \cdot A$ respectively, while the singular values are the square roots of the associated eigenvalues. An approximation of the matrix A is obtained sorting the singular values in a decreasing order and truncating the decomposition (1) to $s < r$ terms, as $A_{ij} \simeq \sum_{l=1}^{s} \delta_l u_{il} v_{jl}$.The error of this approximation in terms of the Frobenius norm $\|A\|^2 = \sum_{i,j} (A_{ij})^2$, is equal to

$$\|error\| = \left[\sum_{l=s+1}^{r} (\delta_l)^2 \right]^{1/2}.$$

When this is appropriately small for a value of s that is much smaller than both m and n, a quite effective compression results. This is because the truncated decomposition requires to save only $s \times (m + n)$ numbers to store the $m \times n$ elements of A. And s will be small when all columns of A are close to linear combinations of a few of them, which in turn will happen when relations are present between the elements of A. Such implicit redundancies can be due to, e.g., physical laws.

The natural extension of SVD to a third-order $(m \times n \times p)$-tensor would be

$$A_{ijk} = \sum_{l=1}^{r} \delta_l u_{il} v_{jl} w_{kl}, \tag{2}$$

where r is known as the rank of the tensor A, defined as the minimum value of r such that the decomposition (2) is possible. However, both the determination of the rank of a tensor and the development of computationally efficient algorithms to calculate minimal decompositions are open problems nowadays [4, 5]. An obvious way to

calculate minimal decompositions is to minimize the Frobenius norm of the difference between the right and left hand sides of (2) for increasing values of r, until that point in which the minimum vanishes. But such problem exhibits multiple local minima and furthermore, calculation of the global minimum is an ill-posed problem [5]. Instead of the decomposition (2), other less restrictive expressions have been tried for tensors. Among them, the HOSVD of the tensor A is of the form

$$A_{ijk} = \sum_{i_1=1}^{r_1} \sum_{j_1=1}^{r_2} \sum_{k_1=1}^{r_3} \sigma_{i_1 j_1 k_1} u_{i i_1} v_{j j_1} w_{k k_1}, \tag{3}$$

where $\sigma_{i_1 j_1 k_1}$ is another third-order tensor, known as the reduced tensor (also called core tensor sometimes), $u_{i i_1}$, $v_{j j_1}$, and $w_{k k_1}$ are again orthonormal, and r_1, r_2, and r_3 are the ranks (defined as usually) of three symmetric positive definite matrices B^1, B^2, and B^3, defined as $B^1_{il} = \sum_{j,k} A_{ijk} A_{ljk}$, $B^2_{jl} = \sum_{i,k} A_{ijk} A_{ilk}$, and $B^3_{kl} = \sum_{i,j} A_{ijk} A_{ijl}$. The HOSVD modes are the eigenvectors associated with the nonzero eigenvalues of the latter matrices, namely,

$$\sum_l B^1_{il} u_{l i_1} = \alpha_{i_1} u_{i i_1}, \quad \sum_l B^2_{jl} v_{l j_1} = \beta_{j_1} v_{j j_1}, \quad \text{and} \quad \sum_l B^3_{kl} w_{l k_1} = \gamma_{k_1} w_{k k_1}. \tag{4}$$

As in the SVD, if the eigenvalues are sorted in a decreasing order, the decomposition (3) can be truncated to the first $s_1 < r_1$, $s_2 < r_2$, and $s_3 < r_3$ modes, as

$$A_{ijk} \simeq \sum_{i_1=1}^{s_1} \sum_{j_1=1}^{s_2} \sum_{k_1=1}^{s_3} \sigma_{i_1 j_1 k_1} u_{i i_1} v_{j j_1} w_{k k_1}, \tag{5}$$

keeping the error (in terms of the Frobenius norm $\|A_{ijk}\|^2 = \sum_{i,j,k} (A_{ijk})^2$) bounded by

$$\|error\| \leq \sqrt{\sum_{i_1=s_1+1}^{r_1} \alpha_{i_1} + \sum_{j_1=s_2+1}^{r_2} \beta_{j_1} + \sum_{k_1=s_3+1}^{r_3} \gamma_{k_1}}. \tag{6}$$

This expression gives an a priori error estimate. The reduced tensor can be calculated multiplying Eq.(3) by $u_{i i_1}$, $v_{j j_1}$, and $w_{k k_1}$, adding in the indexes i_1, j_1, and k_1, and noting that these three systems of vectors are orthonormal. It follows that

$$\sigma_{i_1 j_1 k_1} = \sum_{i=1}^{m} \sum_{j=1}^{n} \sum_{k=1}^{p} A_{ijk} u_{i i_1} v_{j j_1} w_{k k_1}. \tag{7}$$

Note that each element of this tensor requires a number of operations proportional to the size of the original tensor, which can be very large. Thus, it is important to have an a priori estimate of the error that allows to select the number of retained modes to obtain the desired accuracy before computing the reduced tensor. Again, if the bound in (6) is small enough, it is possible to store a good approximation of the original tensor (5) saving $s_1 \times s_2 \times s_3 + s_1 \times m + s_2 \times n + s_3 \times p$ numbers instead of the $m \times n \times p$ elements of A. Compression will be large if s_1, s_2 and/or s_3 are small compared with m, n and/or p, which will happen when the elements of A exhibit approximate redundancies.

Summarizing, a third-order tensor A is decomposed in the form (3), which can be truncated invoking Eq.(6). The HOSVD modes are given by Eq. (4) and the reduced tensor components are calculated using (7). Higher order tensor are treated similarly.

In Aerodynamics, it is common to have tensors when organizing the information on a variable (i.e., the pressure P), as a function of discrete values of parameters and the spatial coordinates; the spatial distributions of the flow variable at these discrete values of the parameters are calculated using CFD and are called snapshots hereafter. Calculation for intermediate parameter values requires interpolation, which in principle can be not efficient when the number of parameters is large. Depending on the application, the number of relevant parameters ranges can be very large. For instance, the aerodynamic flow around a whole airplane involves 7-8 parameters such as the Reynolds and Mach numbers, the angle of attack, the yaw angle, and the deflection angles of the control surfaces (e.g., flaps, ailerons, rudder, and elevator). In these cases, HOSVD both promotes data compression and facilitates interpolation, as we shall see below.

Even though cruise conditions of commercial airplanes are nominally subsonic (Mach number of the order of 0.8), local flow accelerations due to the presence of the aircraft produce regions of supersonic flow. The resulting flow regime is called transonic and exhibits shock waves, which involve jumps in the pressure and other flow variables. Moreover shock waves move as the parameters are varied, which leads to a great difficulty in connection with both HOSVD and interpolation, as we shall see below.

For the sake of clarity, here we consider the discrete pressure distribution over the boundary of a 2-D airfoil, and the effect of only three parameters, namely the Mach number M, the angle of attack α, and the flap deflection angle δ. The airfoil is plotted in Fig.3 below, where the air moves from left to right; thus the downstream and upstream directions essentially indicate right and left in this figure. The upper and lower parts of the airfoil are called suction and pressure sides. Positions along the surface of the airfoil are given by the horizontal coordinate x. The resulting fourth order tensor is decomposed using HOSVD as

$$P_{ijkl} \equiv P(M_i, \alpha_j, \delta_k; x_l) = \sum_{i_1=1}^{r_1} \sum_{i_2=1}^{r_2} \sum_{i_3=1}^{r_3} \sum_{i_4=1}^{r_4} \sigma_{i_1 j_1 k_1 l_1} u_{i i_1} v_{j j_1} w_{k k_1} x_{l l_1}.$$

HOSVD decomposes the influence of each parameter into separated modes. Thus, for intermediate values of the parameters, this decomposition allows to replace the three dimensional interpolation that would be needed in the left hand side by the various onedimensional interpolations that are involved in the right hand side. Namely

$$P_l^* = P(M^*, \alpha^*, \delta^*; x_l) = \sum_{i_1=1}^{r_1} \sum_{i_2=1}^{r_2} \sum_{i_3=1}^{r_3} \sum_{i_4=1}^{r_4} u_{i_1}^* v_{j_1}^* w_{k_1}^* x_{l l_1}, \tag{8}$$

where the superscript $*$ denotes intermediate values. The HOSVD modes associated with the last index are a basis of a linear manifold in the space of possible spatial pressure distributions that effectively approximates the pressure field on the airfoil

surface at any point of the parameter space. The problem is that, if the pressure field exhibits shock waves (or any other localized structure) whose position moves as the values of the parameters are varied, the number of required HOSVD modes (and thus the number of snapshots required to determine them) can be quite large. This is because the final representation of the pressure field is made in terms of linear combinations of HOSVD modes, and linear combinations of pressure fields exhibiting shock waves at different positions can only accurately reconstruct a shock wave if the number of modes is somewhat large compared with the ratio L/d (which is usually quite large), where L is the distance between extreme shock wave positions and d is the shock wave thickness. If this does not hold, the reconstructed shock wave splits the exact jump into combinations of multiple jumps. This is illustrated in Fig.1, where a standard HOSVD (without any a priori treatment of the shock wave) is applied that produces an approximation in which unique pressure jump is replaced by four jumps. The counterpart of this plot resulting from a more convenient method (see next section) is given in Fig.4 below. Note that the same difficulty appears when applying standard interpolation (such as linear or spline interpolation), which is also based on linear combinations, as also illustrated in Fig.1.

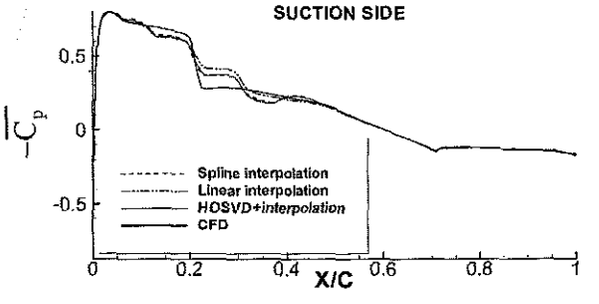

Figure 1: Comparison of the CFD pressure coefficient (a rescaled messure of pressure) and various approximations at $\alpha = 2.25°$, $M = 0.8$, and $\delta = -2.5°$.

3 Shock wave treatment method

The main idea is to extract the shock wave structure from the original pressure distribution, to obtain smoother distributions that are more amenable to HOSVD. The method is organized into three consecutive steps (see Fig.2):

- *Step 1: Identifying the shock wave structure and disassembling.*
  - For each snapshot, we locate that point (Q_3 in Fig.2) exhibiting the largest pressure steepness. If such steepness is smaller than a certain threshold value, it is decided that no shock wave structure is present. Otherwise, Q_3 locates the central position of the shock wave.

– The shock wave region is assumed to extend a few grid points around the central point; six points, $Q_1, \ldots, Q_6$ are involved in the sketch in Fig. 2. This defines the shock wave region (SWR).

– Now, the original pressure distribution is approximated as

$$P \cong P_{jump} + P_{smooth} \tag{9}$$

where P_{jump} essentially accounts for the internal structure of the shock wave and is defined to vanish upstream of the SWR, to behave linearly in the SWR, and be constant (equal to the total pressure jump across the shock wave, ΔP) downstream of the SWR. P_{smooth} instead concides with P upstream the SWR, is constant in the SWR, and equals $P - \Delta P$ downstream of the SWR. Note that P and $P_{jump} + P_{smooth}$ exactly coincide except in the SWR, where a linear approximation is made, which could be improved in various ways. But this is not done here to illustrate the robustness of the results.

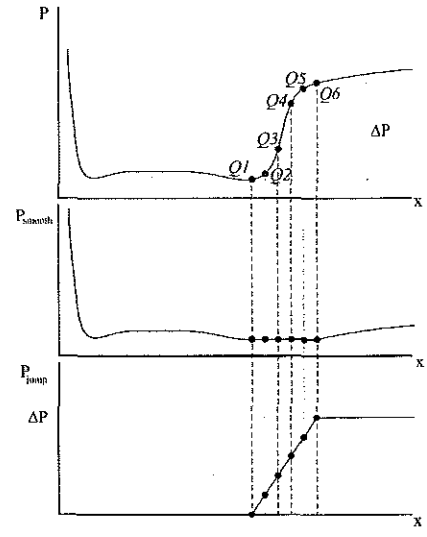

Figure 2: Illustration of the methodology used to treat shock waves

For each value of the parameters, the decomposition below involves the scalars $Q_3(M, \alpha, \delta)$ and $\Delta P(M, \alpha, \delta)$, which define third order tensors, and the spatial distribution $P_{smooth}(x, M, \alpha, \delta)$, a fourth-order tensor. Note that Q_3 and ΔP are only defined at those parameter values for which a shock wave structure exists; ΔP is set to zero at those parameter values where no shock wave structure is present, but Q_3 remains undefined.

- *Step 2: Application of the HOSVD*

- Apply the HOSVD method to the tensors associated with the quantities ΔP and P_{smooth} and truncate the associated decompositions within a specified error using (6).

- *Step 3: Interpolation and assembling of the separated elements*
  - Interpolate the HOSVD modes for the variables ΔP and P_{smooth} as in Eq.(8). Q_3 is not defined in all points of the parameter space so instead of a HOSVD plus interpolation, a local interpolation is performed.
  - The final assembling is made using Eq.(9).

4 Results

The freestream flow around a 2-D isolated airfoil at the fixed Reynolds number of 20×10^6 is considered. Three parameters, namely, the Mach number M, the angle of attack α, and the flap deflection angle δ, are varied in the intervals of $[0.4, 0.8]$, $[-3°, 3°]$, and $[-5°, 5°]$, respectively. Such parameter range includes flow topologies illustrated in Fig.3 that differ significantly from each other. In particular, smooth pressure fields are present at low Mach numbers but other flow topologies show only one shock wave, either in the suction or pressure sides, or two shock waves, one in each side of the airfoil. The method is checked in the 24 test points defined by all the combinations of the following values of the parameters:

- M (3 values): 0.525, 0.725 and 0.8.
- α (4 values): $-2.25°$, $-1.25°$, $1.25°$ and $2.25°$.
- δ (2 values): $-2.5°$ and $2.5°$.

And the method is applied using three different combinations of snapshots which correspond to rectangular meshes in the parameter space with the parameter values indicated below:

- *Combination 1 (*$9 \times 13 \times 9 = 1053$ *snapshots):*
  - $M = 0.4$, 0.45, 0.5, 0.55, 0.6, 0.65, 0.7, 0.75 and 0.8.
  - $\alpha = -3°$, $-2.5°$, $-2°$, $-1.5°$, $-1°$, $-0.5°$, $0°$, $0.5°$, $1°$, $1.5°$, $2°$, $2.5°$, and $3°$.
  - $\delta = -5°$, $-3°$, $-2°$, $-1°$, $0°$, $1°$, $2°$, $3°$ and $5°$.
- *Combination 2 (*$6 \times 9 \times 7 = 378$ *snapshots):*
  - $M = 0.4$, 0.55, 0.65, 0.7, 0.75 and 0.8.
  - $\alpha = -3°$, $-2.5°$, $-1.5°$, $-1°$, $0°$, $1°$, $1.5°$, $2.5°$, and $3°$.
  - $\delta = -5°$, $-3°$, $-2°$, $0°$, $2°$, $3°$ and $5°$.
- *Combination 3 (*$4 \times 5 \times 5 = 100$ *snapshots):*

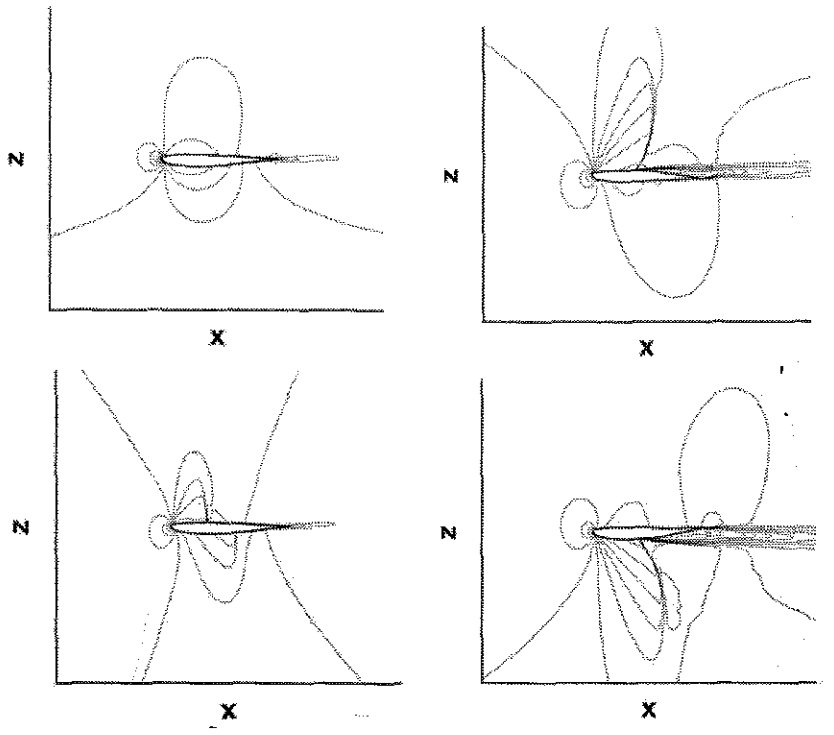

Figure 3: Iso-Mach contours in the $x-z$ plane corresponding to $\alpha = 0°$, $M = 0.4$ and $\delta = 0°$ (top-left); $\alpha = 3°$, $M = 0.8$ and $\delta = 5°$ (top-right); $\alpha = 2°$, $M = 0.8$ and $\delta = -1°$ (bottom-left); $\alpha = -3°$, $M = 0.8$ and $\delta = -5°$ (bottom-right).

- $M = 0.4$, 0.55, 0.7, and 0.8.
- $\alpha = -3°$, $-1.5°$, $0°$, $1.5°$, and $3°$.
- $\delta = -5°$, $-3°$, $0°$, $3°$ and $5°$.

Now, in order to evaluate the approximations we use the lift C_L, momentum C_M, flap momentum C_{FM}, and pressure drag C_{PD} coefficients. These are just some weighted integrals of the pressure along the boundary of the airfoil, see [6]. For illustration, the mean error (ME) in each of these coefficients for all 24 test points are given in Table 1. These results indicate that, in overall terms, the 378 snapshots combination presents the most favorable balance between accuracy and computational cost. Increasing the number of snapshots from 378 to 1053 increases the computational time by a factor of nearly 3 with a very small improvement in accuracy. On the other hand, using 100 snapshots (combination 3), the averaged error increases to the range of $1-3\%$ (which could be still acceptable, for example, in the first steps of the design process, when only estimative values are required). Now, for comparison, C_L, C_M, C_{FM}, C_{PD} are also directly approximated using HOSVD+interpolation to the values of these coefficients calculated from the snapshots, which provides the ME given in Table 2. Comparison

with Table 1 shows that such direct application of HOSVD provides better (but further less detailed) results, as could be expected.

Representative results on local pressure distribution over the 2-D airfoil are summarized in Figs.4–6, which deserve two short comments. First, comparison between Figs.1 and 4 shows that the shock wave treatment method described above solves the problem of reconstructing the local pressure distribution in the vicinity of the shock wave. Second, these figures show that the 378 snapshots combination is again the best in terms of balance between accuracy and computational cost. Combination 3 (only 100 snapshots) instead is not able to calculate the shock wave position in some cases (Fig.5), and is even unable to determine the existence of the shock wave (Fig.6).

	Comb 1	Comb 2	Comb 3
C_L	1.1	2.2	5.0
C_M	2.9	6.0	14.2
C_{FM}	3.8	8.0	20.6
C_D	2.4	5.8	11.4

Table 1: ME errors (%) for all test points when reconstructing global coefficients from local pressure distributions obtained by shock wave treatment and HOSVD+interpolation.

	Comb 1	Comb 2	Comb 3
C_L	0.2	0.3	1.0
C_M	0.6	0.7	2.4
C_{FM}	0.8	0.9	2.5
C_D	0.7	1.1	3.2

Table 2: Counterpart of table 1 applying directly HOSVD+interpolation to the coefficients values at the snapshots.

5 Concluding remarks

A HOSVD-based method, with a preliminary shock wave treatment, has been presented to interpolate in aerodynamic databases. It has been found that our approach is robust and yields results that are dramatically better than those obtained using standard HOSVD + interpolation, as seen comparing Figs. 1 and 4. The removal of the internal structure of the shock wave (see Fig. 2) was made in a fairly rough way. This was done on purpose, to illustrate that the main benefit comes from removing the shock wave structure, and not from the way this is done. Both local and global results are quite good provided that the appropriate number of snapshots are used. It has been found

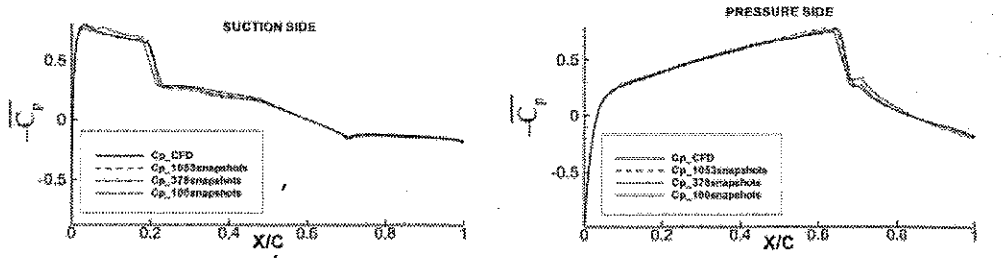

Figure 4: Comparison of the CFD and reconstructed pressure distribution in the case of test point ($\alpha = 2.25°$, $M = 0.8$, and $\delta = -2.5°$).

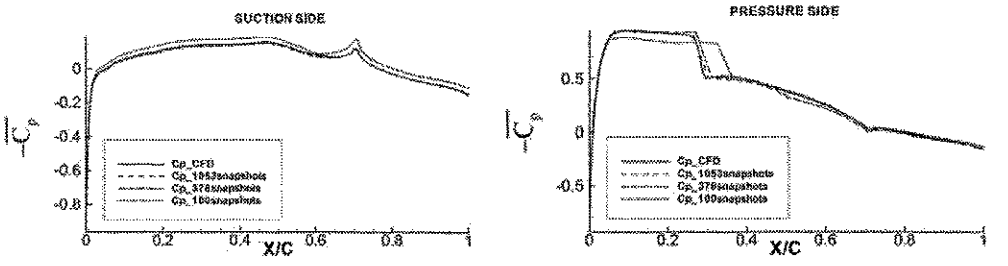

Figure 5: As Fig. 4 in the case of test point ($\alpha = -2.25°$, $M = 0.725$, and $\delta = 2.5°$).

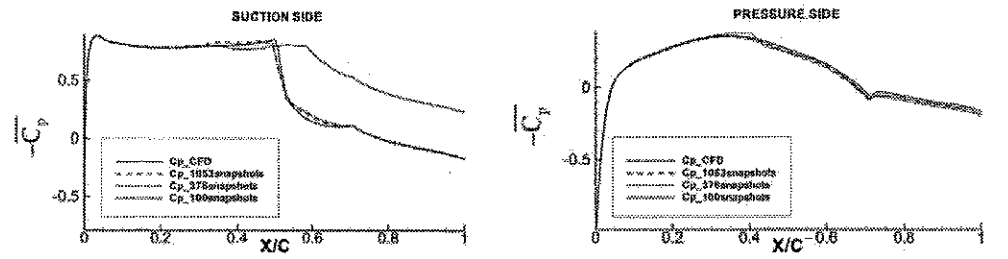

Figure 6: As Fig. 4 in the case of test point ($\alpha = 1.25°$, $M = 0.8$, and $\delta = 2.5°$).

that increasing the amount of information too much (1053 snapshots) does not improve accuracy significantly (CFD errors play role here), whereas getting down too much (100 snapshots) degrades the quality of the results. That is, for a prescribed precision, there is an optimum amount of information that, once reached, does not need improvement. In this frame, the desirable goal, from a practical engineering point of view, would be to be able to estimate this optimum amount of information beforehand. In the test case considered above, the snapshots have been selected in a rectangular, essentially equispaced grid in the parameter space. However, there should be much better strategies. We are working in algorithms to generate databases selecting the snapshots iteratively,

in such a way that they content the largest amount of information possible, minimizing the number of snapshots needed to describe the considered problem.

Finally, concerning practical industrial applications, it has been concluded that a relatively small number of snapshots (combination 3, 100 snapshots) approach 2 delivers global coefficients with an accuracy that could be enough for the early stages of the design process, especially if the coefficients are calculated applying directly HOSVD+interpolation to the coefficients values of the snapshots. If either more accurate information on the global coefficients is required or local pressure information is needed, combination 2 with 378 snapshots provides the required answer. In other words, it is more practical (and less expensive) to work with various different approaches and apply them as required by the industrial environment rather than trying to combine them both in a single "universal tool".

Acknowledgements

This research project has been funded by Airbus (contract A8208636G). One of the authors, J.M. Vega, has also been partially supported by the Spanish Ministry of Education (Grant TRA2007-65699/TAIR). The authors are indebted to Carlos Artiles and Valentín de Pablo, of Airbus, for their continuous guidance in the precise identification of the relevant requirements of the method in terms of daily engineering needs and to Markus Wikdham of the DLR for his assistance with the CFD computations.

References

[1] T. Bui-Thanh, *Proper orthogonal decomposition extensions and their applications in steady aerodynamics*, Master's Thesis, Singapore-Massachusetts Institute of Technology Alliance (2003).

[2] L. S. Lorente, J. M. Vega, and A. Velazquez, *Generation of aerodynamic databases using high-order singular value decomposition*, J. Aircraft **45** (2008) 1779–1788.

[3] L. de Lathauwer, B. de Moor, and J. Vandewalle, *A multilinear singular value decomposition*, SIAM J. Matrix Anal. Appl. **21** (2000) 1253–1278.

[4] L. de Lathauwer, B. de Moor, and J. Vandewalle, *On the best rank-one and rank-$(R_1, R_2, \ldots, R_N)$ approximation of higher order tensors*, SIAM J. Matrix Anal. Appl. **21** (2000) 1324–1342.

[5] V. da Silva and L. H. Lim, *Tensor rank and the ill-posedness of the best low-rank approximation problem*, SIAM J. Matrix Anal. Appl. **30** (2008) 1084–1127.

[6] J.D. Anderson, *Fundamentals of Aerodynamics*, McGraw Hill (2007).